

**RADIATION SHIELDING AND OPTICAL  
PROPERTIES OF ADDED BAO AND WO<sub>3</sub> TO  
BI<sub>2</sub>O<sub>3</sub>-ZNO-B<sub>2</sub>O<sub>3</sub>-SLS GLASS NETWORK AT  
SELECTIVE PHOTON ENERGY**

**THAIR HUSSEIN ABEDALRAHMAN  
KHAZAALAH**

**UNIVERSITI SAINS MALAYSIA**

**2023**

**RADIATION SHIELDING AND OPTICAL  
PROPERTIES OF ADDED BAO AND WO<sub>3</sub> TO  
BI<sub>2</sub>O<sub>3</sub>-ZNO-B<sub>2</sub>O<sub>3</sub>-SLS GLASS NETWORK AT  
SELECTIVE PHOTON ENERGY**

by

**THAIR HUSSEIN ABEDALRAHMAN  
KHAZAALAH**

**Thesis submitted in fulfilment of the requirements  
for the degree of  
Doctor of Philosophy**

**April 2023**

## ACKNOWLEDGEMENT

In the name of Allah, the Most Gracious and the Most Merciful.

Alhamdulillah, I am grateful to Allah S.W.T who gave me the courage and strength to complete this research in due time. It is a great pleasure to acknowledge my deepest thanks and gratitude to Dr. Iskandar Shahrin Mustafa for suggesting the topic of this thesis and for his scientific as well as moral support, guidance, and encouragement throughout this research journey. It was very special experience to work with Dr. Iskandar Shahrin Mustafa and I learned valuable academic skills from his instructions. Also, I would like to express my deepest gratitude to my friend Dr. M.I. Sayyed for his encouragement, guidance, and support throughout this journey.

Last but not least, this work could not have existed without the inspiration, support, and love of my father, my mother, my brothers, and my sisters. I would not have been able to complete this work without their help. My sincere appreciation and thanks are extended to all my friends in Jordan and Malaysia for supporting me to achieve my goal. I am grateful to every who contributed either directly or indirectly to my work to achieve my goal. Thank you.

Thair Hussein Khazaalah

## TABLE OF CONTENTS

<b>ACKNOWLEDGEMENT .....</b>	<b>ii</b>
<b>TABLE OF CONTENTS.....</b>	<b>iii</b>
<b>LIST OF TABLES .....</b>	<b>vi</b>
<b>LIST OF FIGURES .....</b>	<b>viii</b>
<b>LIST OF SYMBOLS .....</b>	<b>xxii</b>
<b>LIST OF ABBREVIATIONS .....</b>	<b>xxiii</b>
<b>ABSTRAK .....</b>	<b>xviii</b>
<b>ABSTRACT .....</b>	<b>xvi</b>
<b>CHAPTER 1 INTRODUCTION.....</b>	<b>1</b>
1.1 Background .....	1
1.2 Problem Statement .....	3
1.3 Objectives.....	5
1.4 Scope of Study .....	5
1.5 Outline of Thesis .....	6
<b>CHAPTER 2 LITERATURE REVIEW.....</b>	<b>7</b>
2.1 Radiation Background.....	7
2.1.1 Introduction.....	7
2.1.2 Photon interaction with matter .....	9
2.1.2(a) The photoelectric effect.....	10
2.1.2(b) Compton scattering .....	10
2.1.2(c) Pair production .....	11
2.2 The glass as radiation shielding materials.....	11
2.3 Radiation shielding parameters .....	13
2.3.1 Linear attenuation coefficient .....	13
2.3.2 Mass attenuation coefficient .....	14

2.3.3	Half-Value Layer (HVL) and mean free path (MFP) .....	18
2.3.4	The effective atomic number ( $Z_{eff}$ ) and electron density ( $N_{el}$ ) ....	20
2.3.5	Radiation protection efficiency (RPE).....	22
2.4	Attenuation study in theoretical approach.....	23
2.5	Study of Soda Lime Silica (SLS) Glass .....	24
2.6	The Physical Properties .....	25
2.7	X-ray Diffraction (XRD).....	29
2.8	Optical properties of glass.....	32
<b>CHAPTER 3 METHODOLOGY.....</b>		<b>41</b>
3.1	Research design.....	41
3.2	Glass samples preparation .....	41
3.3	Measurements.....	44
3.3.1	Physical properties .....	44
3.3.2	XRD .....	44
3.3.3	EDX .....	45
3.3.4	Measurement of transmitted gamma-ray .....	45
3.3.5	Optical measurement.....	47
<b>CHAPTER 4 RESULT AND DISSCUSION.....</b>		<b>50</b>
4.1	Soda Lime Silica (SLS) glass waste contents .....	50
4.2	Structural properties .....	51
4.2.1	XRD .....	51
4.2.2	EDX .....	53
4.3	The physical properties .....	55
4.4	Radiation shielding features: experimental approach .....	61
4.4.1	Calibration curve.....	61
4.4.2	Attenuation coeficient parameters. ....	62
4.4.3	Half value layer (HVL), mean free path (MFP), effective atomic number ( $Z_{eff}$ ), and effective electron number ( $N_{el}$ ).....	70

4.5	Radiation shielding features: theoretical approach .....	71
4.6	Optical measurements of glass .....	77
<b>CHAPTER 5 CONCLUSION AND FUTURE RECOMMENDATIONS .....</b>		<b>91</b>
5.1	Conclusion.....	91
5.2	Recommendations for Future Research .....	94
<b>REFERENCES.....</b>		<b>96</b>
<b>APPENDICES</b>		
<b>LIST OF PUBLICATIONS</b>		

## LIST OF TABLES

		<b>Page</b>
Table 2.1	Summery of the literature review .....	40
Table 3.1	Detailes of chemical powder used.....	42
Table 3.2	Glass composition concentration .....	44
Table 3.3	Metal plates used in X-ray fluorescenc (XRF) confeguration .....	45
Table 4.1	Elemants included in Soda-Lime- silica (SIS) glass waste .....	51
Table 4.2	he analysis data from EDX of CS, W1, W3, W5, Ba1, Ba3, and Ba5 glass .....	54
Table 4.3	Density ( $\rho$ ), molar volume( $V_m$ ), and oxygen packing density (OPD) of fabricated glass samples .....	56
Table 4.4	Ion concentration (N), internuclear distance ( $r_i$ ), polaron radius ( $r_p$ ), and field strength (F) of fabricated glass samples.....	60
Table 4.5	Linear attenuation coefficient ( $\mu$ ) of current glass samples .....	64
Table 4.6	Mass attenuation coefficient ( $\mu_m$ ) and radiation protection efficiency of current glass samples .....	67
Table 4.7	Mass attenuation coefficient of some concrete and glass samples at 59.54 662, and 1333 keV .....	68
Table 4.8	Half value layer (HVL) and mean free path (MFP) of the current glass samples.....	70
Table 4.9	Effective atomic number ( $Z_{eff}$ ) and electron density ( $N_{el} \times 10^{23}$ ) electron g-1 of glass samples .....	71
Table 4.10	Linear attenuation coefficient value from experimental and theoretical for glass samples .....	76
Table 4.11	Indirect and direct energy band gaps, Urbach energy, refraction and molar referactive indices of glass samples .....	81

Table 4.12	Metallization, molar electronic polarizability, optical basicity, dielectric constant, reflection loss, and transmission of the fabricated glass samples .....	84
Table B.1	Molecular weight (g/mol) of glass mixture.....	110
Table B.2	The subtotal weight percentage of WO <sub>3</sub> glass samples.....	110
Table B.3	The weight (g) of WO <sub>3</sub> glass samples .....	110
Table B.4	The subtotal weight percentage of BaO glass samples .....	111
Table B.5	The weight (g) of BaO glass samples .....	111
Table B.6	The detail of the radioactive source .....	111
Table B.7	Mass attenuation coefficient of WO <sub>3</sub> glass samples (PhysX/SPD) software.....	112
Table B.8	Mass attenuation coefficient of BaO glass samples (PhysX/SPD) software.....	113
Table B.9	Half value layer of WO <sub>3</sub> glass samples (PhysX/SPD) software.....	114
Table B.10	Half value layer of BaO glass samples (PhysX/SPD) software.....	115
Table B.11	Effective atomic number of WO <sub>3</sub> glass samples (PhysX/SPD) software.....	116
Table B.12	Effective atomic number of BaO glass samples (PhysX/SPD) software.....	117

## LIST OF FIGURES

		<b>Page</b>
Figure 2.1	XRD analysis of WO <sub>3</sub> -PbO-Bi <sub>2</sub> O <sub>3</sub> -B <sub>2</sub> O <sub>3</sub> glass samples (Chen,2019).....	11
Figure 2.2	Varaiation of density and molar volume of BaO-Bi <sub>2</sub> O <sub>3</sub> -P <sub>2</sub> O <sub>5</sub> glass system (El-Bashir et al.,2017).....	14
Figure 2.3	Density and molar volume as a function of mole fraction for (a) Bi <sub>2</sub> O <sub>3</sub> and (b) PbO (Ahamad et al.,2019).....	15
Figure 2.4	Type of radiation and their ability to penetrate.....	17
Figure 2.5	The three major types of radiation interactions with matter (Knoll,2010).....	18
Figure 2.6	Variation of linear attenuation coefficient (LAC) with photon energy (El-Denglawey et al.,2021).....	154
Figure 2.7	Variation of mass attenuation coefficient (MAC) values foe the glass samples with photon energy (El-Denglawey et al.,2021).....	215
Figure 2.8	The HVL of fabrication glasses with energy (Abouhousa et al.,2022b).....	227
Figure 2.9	The effective atomic number of the glass samples against incoming photon energy (Teresa et al.,2021).....	30
Figure 2.10	The dependence of $(\alpha h\nu)^2$ and $(\alpha h\nu)^{1/2}$ on the photon energy (Abuhaswa et al.,2020a).....	35
Figure 2.11	Refractive index and optical energy gap for barium borate glasses (Ali et al.,2020).....	37
Figure 2.12	Reflection loss and optical transmission for PbO-TeO <sub>2</sub> (Elazoumi et al.,2018).....	39
Figure 3.1	Methodology current research.....	41
Figure 3.2	Glass samples preparation steps.....	43

Figure 3.3	Glass samples of WO <sub>3</sub> and BaO doped in Bi <sub>2</sub> O <sub>3</sub> -ZnO-B <sub>2</sub> O <sub>3</sub> -SLS glass.....	43
Figure 3.4	Setup for X-rar flourescence (XRF).....	46
Figure 3.5	Setup of narrow beam geometry .....	47
Figure 3.6	PhysX/SPD online software.....	48
Figure 3.7	The diagram of UV-Visible spectrophotometer.....	49
Figure 4.1	XRD patterns of WO <sub>3</sub> glass samples.....	52
Figure 4.2	XRD patterns of BaO glass samples .....	52
Figure 4.3	EDX spectra of W1 and W5 glass samples.....	53
Figure 4.4	EDX spectra of Ba3 and Ba5 glass samples .....	54
Figure 4.5	Density and molar volume of fabricated glass samples against WO <sub>3</sub> concentrations.....	56
Figure 4.6	Density and molar volume of fabricated glass samples against BaO concentrations .....	57
Figure 4.7	Oxygen packing density and molar volume of fabricated glasses against WO <sub>3</sub> concentrations .....	58
Figure 4.8	Oxygen packing density and molar volume of fabricated glasses against BaO concentrations.....	59
Figure 4.9	Standard calibriation curve .....	61
Figure 4.10	Linear attenuation coefficient of prepared glasses.....	64
Figure 4.11	Mass attenuation coefficient of prepared glasses.....	66
Figure 4.12	Comparsion of $\mu_m$ values of the present study with the $\mu_m$ of other concrete and glass samples at 59.54 keV .....	67
Figure 4.13	Half-value layer of glass samples .....	69
Figure 4.14	Mean free path of glass samples .....	69
Figure 4.15	The effective atomic number of glass samples .....	71
Figure 4.16	Mass attenuation coefficient of glass samples from PhysX\SPD software results.....	72

Figure 4.17	The relationship between the $\mu$ values and HVL values of W5 against photon energy .....	73
Figure 4.18	Hlaf-value layer of glass samples from PhysX/SPD software results .....	74
Figure 4.19	Comparasion of the HVL results of current work with previous studies.....	74
Figure 4.20	Effective atomic number of glass samoles from PhysX/SPD software result .....	75
Figure 4.21	The UV-Vis absorbance spectrum of WO <sub>3</sub> doped with Bi <sub>2</sub> O <sub>3</sub> -ZnO-B <sub>2</sub> O <sub>3</sub> -SLS glass .....	78
Figure 4.22	The UV-Vis absorbance spectrum of BaO doped with Bi <sub>2</sub> O <sub>3</sub> -ZnO-B <sub>2</sub> O <sub>3</sub> -SLS glass .....	78
Figure 4.23	Part of direct band $gap(\alpha h\nu)^2$ of WO <sub>3</sub> doped with Bi <sub>2</sub> O <sub>3</sub> -ZnO-B <sub>2</sub> O <sub>3</sub> -SLS glass.....	79
Figure 4.24	Part of indirect band $gap(\alpha h\nu)^{1/2}$ of WO <sub>3</sub> doped with Bi <sub>2</sub> O <sub>3</sub> -ZnO-B <sub>2</sub> O <sub>3</sub> -SLS glass .....	80
Figure 4.25	Part of direct band $gap(\alpha h\nu)^2$ of BaO doped with Bi <sub>2</sub> O <sub>3</sub> -ZnO-B <sub>2</sub> O <sub>3</sub> -SLS glass.....	80
Figure 4.26	Part of indirect band $gap(\alpha h\nu)^{1/2}$ of BaO doped with Bi <sub>2</sub> O <sub>3</sub> -ZnO-B <sub>2</sub> O <sub>3</sub> -SLS glass .....	81
Figure 4.27	Urbach energy of prepared glass samples.....	82
Figure 4.28	Refractive index of prepared glass samples .....	83
Figure 4.29	Molar polaraizability and molar electron polarizability versus the molar referactive index for WO <sub>3</sub> -glass.....	85
Figure 4.30	Molar polaraizability and molar electron polarizability versus the molar referactive index for BaO-glass .....	86
Figure 4.31	The relationship between Eopt and $\Lambda$ against WO <sub>3</sub> cnotent .....	87
Figure 4.32	The relationship between Eopt and $\Lambda$ against BaO cnotent.....	88

Figure 4.33	The behaviour of dielectric constant and optical dielectric constant against WO <sub>3</sub> content.....	89
Figure 4.34	The behaviour of dielectric constant and optical dielectric constant against BaO content .....	89
Figure 4.35	Transmission and reflection loss for WO <sub>3</sub> -glass samples .....	90
Figure 4.36	Transmission and reflection loss for BaO-glass samples.....	90
Figure A.1	Measurement of density device.....	108
Figure A.2	XRD device.....	108
Figure A.3	EDX device .....	109
Figure A.4	UV-Vis spectrometer .....	109
Figure A.5	$\gamma$ -ray spectrometer.....	109

## LIST OF SYMBOLS

$M$	Metallization criterion
$M_{wt}$	Molecular weight
$n$	Refractive index
$N_A$	Avogadro's number ( $6.0228 \times 10^{23} \text{ g mol}^{-1}$ )
$N_{el}$	Effective electron number
$R_L$	Reflection loss
$T$	Transmission coefficient
$V_m$	Molar volume
$Z_{eff}$	Effective atomic number
$\alpha_m$	Molar polarizability
$\Delta E$	Urbach energy
$\gamma$	Gamma-ray
$\lambda$	Wavelength
$\Lambda$	Optical basicity
$\mu$	Linear attenuation coefficient
$\mu_m$	Mass attenuation coefficient
$\rho$	Density
$\varepsilon$	Dielectric constant

## LIST OF ABBREVIATIONS

BaO	Barium Oxide
B <sub>2</sub> O <sub>3</sub>	Boron Trioxide
Bi <sub>2</sub> O <sub>3</sub>	Bismuth (II) Oxide
BO	Bridging Oxygen
EDX	Energy Dispersive X-ray spectroscopy
HMO	Heavy Metal Oxide
HVL	Half Value Layer
MFP	Mean Free Path
NBO	Non-Bridging Oxygen
OPD	Oxygen Packing Density
PE	Photoelectric Effect
RPE	Radiation Protection Efficiency
SLS	Soda Lime Silica
WO <sub>3</sub>	Tungsten Trioxide
XRD	X-ray Diffraction
XRF	X-ray Fluorescence
ZnO	Zinc Oxide

**PERISAIAN SINARAN DAN PENCIRIAN OPTIK UNTUK TAMBAHAN  
BAO DAN WO<sub>3</sub> PADA RANGKAIAN KACA BI<sub>2</sub>O<sub>3</sub>-ZNO-B<sub>2</sub>O<sub>3</sub>-SLS PADA  
TENAGA FOTON TERPILIH**

**ABSTRAK**

Dalam kajian semasa, WO<sub>3</sub> dan BaO telah di dopkan di dalam kaca Bi<sub>2</sub>O<sub>3</sub>-ZnO-B<sub>2</sub>O<sub>3</sub>-SLS untuk menghasilkan perlindungan radiasi yang bebas plumbum dan menyelesaikan masalah warna kaca Bismuth yang perang gelap. Tambahan pula, lebih kaca silika kapur soda (SLS) telah digunakan bagi menghadkan penambahan dalam pembaziran kaca, dimana ia memerlukan masa yang lama untuk diuraikan. Ini juga dapat menjimatkan penggunaan SiO<sub>2</sub> tulen, dimana ia merupakan sumber terbatas. Kaedah sepuh lindap dimanfaatkan membuat sebelas sampel kaca. Ciri-ciri struktur, fizikal, optic, dan Pengecilan sample kaca semasa telah dipelajari. Keputusan XRF menunjukkan bahawa lebih kaca SLS mengandungi pelbagai sebtain kimia seperti 74.1% SiO<sub>2</sub> dan juga unsur-unsur lain. XRD menunjukkan bahawa semua sample kaca tersebut adalah semulajadi amorfus kerana ketiadaan puncak yang tajam dan garis diskret. Keputusan fizikal menunjukkan bahawa nilai isipadu sample kaca WO<sub>3</sub> menaik daripada 5.229 kepada 5.311 gcm<sup>-3</sup> manakala isipadu molar tetap kekal dengan kenaikan dalam kepekatan WO<sub>3</sub>. Selain itu, hubungan diantara ketumpatan dan isipadu molar bagi struktur kaca BaO adalah songsang. Pengecilan parameter radiasi telah dilakukan secara eksperimental menggunakan XRF dan sinaran geomeri yang sempit. Pekali pengecilan linear pada Kawasan tenaga rendah telah menaik daripada 14.170 kepada 14.281 cm<sup>-1</sup> dengan kepekatan WO<sub>3</sub> juga menaik, manakanilai  $\mu$  bagi kaca BaO telah meningkat daripada 10.319 kepada 11.167 cm<sup>-1</sup>. Selain itu, Half-Value Layer (HVL) dan Mean

Free Path (MFP) telah dikurangkan apabila kepekatan  $\text{WO}_3$  dan  $\text{BaO}$  dinaikkan. Nilai HVL dan MFP bagi kaca tungsten adalah kurang daripada kaca Barium pada 59.54 dan 662 keV, manakala keputusan bagi kaca  $\text{BaO}$  adalah kurang daripada kaca  $\text{WO}_3$  pada 1333 keV. Ciri-ciri optic telah disiasat dengan bantuan spectrometer UV. Keputusan bagi ciri-ciri optic telah membuktikan bahawa apabila kepekatan  $\text{WO}_3$  dan  $\text{BaO}$  meningkat dalam struktur kaca, tenaga Urbach ( $\Delta E$ ), indeks pembiasan ( $n$ ), dan kebesaran optik ( $\Lambda$ ), dalam masa sama jurang jalur optik ( $E_{\text{opt}}$ ) berkurang bagi peralihan electron secara langsung dan tidak langsung. Tambahan pula, kriteria penglogaman ( $M$ ) mengesahkan bahawa sample kaca adalah bukan logam (insulator) kerana  $R_m/V_m \leq 1$ , dimana ini membuktikan didalam teori jirim termampat yang ada dalam persamaan Lorentz-Lorenz.

**RADIATION SHIELDING AND OPTICAL PROPERTIES OF ADDED BAO  
AND WO3 TO BI2O3-ZNO-B2O3-SLS GLASS NETWORK AT SELECTIVE  
PHOTON ENERGY ABSTRACT**

**ABSTRACT**

In the current study, WO<sub>3</sub> and BaO were added to Bi<sub>2</sub>O<sub>3</sub>-ZnO-B<sub>2</sub>O<sub>3</sub>-SLS glass to develop lead-free radiation shielding glasses and solve bismuth glass's dark brown. Furthermore, the Soda-Lime-Silica (SLS) glass waste used to limit the accumulation glass waste, which requires extensive time to decompose. This also saves on the consumption of pure SiO<sub>2</sub>, which is a finite resource. The melt-quenching method was utilized to fabricate eleven glass samples. The structural, physical, optical, and attenuation characteristics were studied for current glass samples. The XRF results showed that SLS waste glass contained multi-chemical compounds such as 74.1% SiO<sub>2</sub> and other minor elements. The physical results indicated that the density values of the WO<sub>3</sub>-glass samples rose gradually from 5.229 to 5.311 gcm<sup>-3</sup> while the molar volume remained constant with the increase in WO<sub>3</sub> content. Also, the relationship between density and molar volume of the BaO-glass network was inverse. The radiation attenuation parameters were experimentally computed using the X-ray fluorescence technique (XRF) and narrow beam geometry. The linear attenuation coefficient ( $\mu$ ) at the low energy region was increased from 14.170 to 14.281 cm<sup>-1</sup> as WO<sub>3</sub> content was increased, while the  $\mu$  values of BaO glass were increased from 10.319 to 11.167 cm<sup>-1</sup>. Furthermore, the half-value layer (HVL) and mean free path (MFP) were reduced when the concentration of WO<sub>3</sub> and BaO was raised. The HVL and MFP values of tungsten glass were less than those of

barium glass at 59.54 and 662 keV, while the results of BaO glass were less than those of WO<sub>3</sub> glass at 1333 keV. The optical properties were investigated with the help of a UV–Visible Spectrophotometer. The results for the optical properties showed that when WO<sub>3</sub> and BaO content was increased in the glass structure, the Urbach energy ( $\Delta E$ ), refractive index ( $n$ ), and the optical basicity ( $\Lambda$ ) increased, while the energy optical band gap ( $E_{opt}$ ) registered a decrease in both electron transition direct and indirect. In addition, the metallization criterion ( $M$ ) confirmed that the current glass samples are non-metallic (insulators) because  $R_m/V_m \leq 1$  which is confirmed in the condensed matter theory in the Lorentz–Lorenz equations.

# CHAPTER 1

## INTRODUCTION

### 1.1 Background

Nuclear applications are becoming more prevalent in our daily lives as a result of their many advantages. They are employed in many fields, such as industry, agriculture, medicine, and radiology, and are used to generate clean energy instead of fossil fuels. However, there are a lot of critical side effects for patients and employees exposed to radiation when they are exposed to high doses of radiation, particularly ionizing radiation, such as DNA damage and mutations. This leads to an increased risk of cancer. In addition, when the lens of the eye is exposed to a high radiation dose, it will cause vision loss because of corneal opacity. Furthermore, men and women who get a lot of ionizing radiation in their bodies will become sterile. As a result, researchers in the developing shielding materials field are interested in developing radiation shield materials to reduce health risk (Albarzan et al., 2021; Al-Yousef et al., 2021; Stalin et al., 2021).

Lead, concrete, ceramics, and polymers are some of the best shielding materials. Concrete is considered to be a conventional and economical technique used for shielding purposes. It is efficient and cheap, and can be easily shaped into any desired design. However, there are some limitations related to concrete, such as its opacity, preventing visible light from passing through, and its mechanical strength being reduced when exposed to radiation for a longer period of time (Kruželák, Kvasničáková, Hložeková, & Hudec, 2021; Roslan, Ismail, Kueh, & Zin, 2019).

Currently, glass is a type of radiation shielding material that can be used instead of opaque shielding materials to protect against radiation risks. It has great chemical and physical properties, such as excellent optical transparency to visible light, ease of production, non toxicity, and low cost. Its physical properties, such as density and effective atomic number, can be changed by adding heavy metal oxides to the glass network.

Researchers working on glass shielding materials used heavy metal oxides such as PbO, Bi<sub>2</sub>O<sub>3</sub>, BaO, and other modifiers in the glass structure to improve the ability of glass to absorb and attenuate radiation. Recently , Researchers switched to using eco-friendly materials instead of PbO due to lead toxicity, and they classified Bi<sub>2</sub>O<sub>3</sub> glass as an ideal candidate for radiation protection. Due to the fact that Bi<sub>2</sub>O<sub>3</sub> is very dense, has a high effective atomic number, a high refractive index, long infrared transmission, and is not toxic. Many research groups have confirmed that the ability of Bi<sub>2</sub>O<sub>3</sub> glass to attenuate photons is enhanced with the increase in the content of Bi<sub>2</sub>O<sub>3</sub> (Dong et al., 2017; Sayyed, Kaky, Mhareb, et al., 2019).

Some parameters related to attenuation such as linear and mass attenuation coefficient, half value layer, mean free path, radiation protection efficiency, and effective atomic number are calculated for estimating the radiation shielding properties when designing radiation shields for X and gamma rays. The effective atomic number is considered a very useful parameter for mixture materials such as glass. The research teams are working on developing lead-free glass shielding, in other words, using eco-friendly materials instead of lead.

The radioactive source Am-241, which has a gamma emission of 59.54 keV, is used in both industrial and diagnostic medical imaging applications. Cs-137 (662 keV) is employed in the medical field as a kind of radiotherapy, which is a type of treatment that makes use of ionizing radiation and is often used for the treatment of cancer in order to control or destroy malignant cells. While the radioisotope Co-60 (1.333 MeV) is one of the most frequently used radioisotopes in industry and medicine, it is also used in industrial radiography, gamma sterilization, and treating cancer by irradiating the affected areas of the body.

Manufacturing industries play a significant role in economic growth. Soda lime silica (SLS) glass is one of the most widely used industrial glass products, accounting for up to 90–95% of global glass production, and is used for flat glass or container wares and windowpanes. Furthermore, SLS glass has significant properties compared to other conventional glass due to its unique properties such as excellent chemical, optical and mechanical properties like low thermal expansion coefficient, nonlinear refractive index, fine chemical stability, high UV transparency, large tensile fracture strength, good electrical resistivity, low production costs, and good durability for optics applications. This industrialization produces an enormous amount of solid waste that causes environmental problems due to the accumulation of waste and limited landfill sites(Almasri, Matori, Zaid, et al., 2017; Dong et al., 2018; Kurtulus & Kavas, 2020).

## **1.2 Problem Statement**

One of the heavy metal oxide glasses is  $\text{Bi}_2\text{O}_3$  glass. Due to its unique characteristics like high density, high atomic number, and others,  $\text{Bi}_2\text{O}_3$  glass is

considered to be a suitable alternative to toxic PbO glasses for use in radiation shielding implementations. Bi<sub>2</sub>O<sub>3</sub> glass's ability to reduce photon intensity increases with Bi<sub>2</sub>O<sub>3</sub> content in the glass network increasing (Cheewasukhanont, Limkitjaroenporn, Kothan, Kedkaew, & Kaewkhao, 2020; Sanz, Haro-Poniatowski, Gonzalo, & Navarro, 2006). However, there are a few issues with the use of high concentrations of Bi<sub>2</sub>O<sub>3</sub> (more than 25% mol) in the glass network, such as the color of the glass becoming dark brown or black and the melting temperature increasing. As a result, researchers in the materials sciences and glass developers have a technical problem in developing Bi<sub>2</sub>O<sub>3</sub> glass that possesses high radiation protection and high transmission (Sanz et al., 2006). Hence, this thesis will provide assistance in solving this problem by using WO<sub>3</sub> and BaO with 20% mol of Bi<sub>2</sub>O<sub>3</sub> to prepare two series of glass compositions, which are WO<sub>3</sub>-glass and BaO-glass. in order to improve attenuation properties.

Soda lime silica (SLS) glass is one of the types of glass with a higher production rate in many fields. In addition to the good optical and mechanical characteristics of SLS glass waste, such as high thermal stability, high transparency, low melting point, and perfect chemical stability (Bateni, Hamidon, & Matori, 2014; M. H. M. Zaid, Matori, Ab, Wahab, & Rashid, 2017). However, SLS glass waste needs a long time to decompose in addition to the limited landfill sites. This contributes to the accumulation of glass waste. To solve environmental problems, researchers are interested in reusing glass waste as an alternative source of SiO<sub>2</sub>. SLS is composed of SiO<sub>2</sub>, Na<sub>2</sub>O, CaO, MgO, Al<sub>2</sub>O<sub>3</sub>, and other elements (Sayed, Elmahroug, Elbashir, & Issa, 2017). The reusing of SLS glass waste as a source of SiO<sub>2</sub> reduces production costs, so this thesis will provide a method for the disposal of SLS waste glass in order to reduce production

costs, save natural resources, limit waste accumulation, and use SLS waste to become a shielding material against radiation.

### 1.3 Objectives

- Developing radiation-shielding glass materials using non-toxic materials such as  $\text{Bi}_2\text{O}_3$ ,  $\text{WO}_3$ , and  $\text{BaO}$  for use as radiation protection equipment in the control room for the reactor and radiotherapy room.
- Using SLS waste glass as an alternative to  $\text{SiO}_2$  to reduce production costs, save natural resources, and limit waste accumulation. The aims of study as follows:
- Measuring the physical and structural properties of  $\text{WO}_3\text{-Bi}_2\text{O}_3\text{-ZnO-B}_2\text{O}_3\text{-SLS}$  glass and  $\text{BaO-Bi}_2\text{O}_3\text{-ZnO-B}_2\text{O}_3\text{-SLS}$  glass.
- Analyzing the optical properties of  $\text{WO}_3\text{-Bi}_2\text{O}_3\text{-ZnO-B}_2\text{O}_3\text{-SLS}$  glass and  $\text{BaO-Bi}_2\text{O}_3\text{-ZnO-B}_2\text{O}_3\text{-SLS}$  glass.
- Evaluating the radiation shielding parameterization of the prepared glass samples at selective photon energy experimentally and theoretically.

### 1.4 Scope of Study

In the current study, the author use the melt-quenching method to fabricate two series of glasses at  $1200^\circ\text{C}$  after studying the melting point for each element in the composition. Soda lime silica glass waste (SLS), which is mostly composed of  $\text{SiO}_2$ ,  $\text{Na}_2\text{O}$ ,  $\text{CaO}$ , and other elements, was used to obtain  $\text{SiO}_2$ . Furthermore, the eco-friendly heavy metal oxides were used to fabricate glass.

XRD analysis will determine the crystal structure of the prepared glass samples

(sharp peaks or broad hump). And, EDX will determine the chemical content of the prepared glass. Furthermore, the attenuation parameters of glass samples will be measured using narrow beam geometry in the energy range (59.54, 662, and 1333 keV). In the meantime, an UV–Visible Spectrophotometer will be used to measure the optical parameters between 200 and 800 nm.

On the other hand, using PhysX/PSD software, the main radiation shielding parameters of glass samples will be theoretically calculated in the energy range of (0.0138–15) MeV.

## **1.5 Outline of Thesis**

In the first chapter, the author presents an overview of the project, including background, problem statement, objectives, the scope of the study, and significance. while chapter two shows a literature review related to this thesis. Chapter three depicts the research methodology and experimental procedure method. Chapter four discusses the experimental results, which included physical, structural, and optical properties of current glass samples. Besides the gamma attenuation parameterization, which will be measured theoretically and experimentally, Finally, chapter five gives a conclusion and summary of this thesis, and it shows a recommendation and future study of  $\text{WO}_3\text{-Bi}_2\text{O}_3\text{-ZnO-B}_2\text{O}_3\text{-SLS}$  glass and  $\text{BaO-Bi}_2\text{O}_3\text{-ZnO-B}_2\text{O}_3\text{-SLS}$  glass.

## **CHAPTER 2**

### **LITERATURE REVIEW**

#### **2.1 Radiation background**

##### **2.1.1 Introduction**

Radiation is defined as the energy that is emitted from a source and passes through space penetrating a variety of materials. There are two forms of radiation: non-ionizing radiation and ionizing radiation. Non-ionizing radiation is also known as low-energy radiation. It lacks sufficient energy to remove an electron from a molecule or atom, such as infrared radiation, visible light, and ultraviolet (UV) radiation. Ionizing radiation has high energy and can excite and ionize electrons in atom or molecule. It can be classified into two groups: charged particles like alpha and beta particles, and protons. Uncharged particles such as X-rays, gamma-rays, and neutron (Tsoulfanidis & Landsberger, 2021).

There are three factors that can be used to manage the radiation dose at a safe level, such as time, distance, and shielding. Time is an essential part of reducing radiation exposure. When a person is exposed to radiation for a longer period of time, a greater amount of radiation will be absorbed into their bodies, which will result in a higher overall radiation dosage. The distance can be used to limit the intensity of radiation between the radiation source and the worker who uses the radiation. According to the inverse square law, there is an inverse relationship between radiation dose and distance. The exposure is decreased by a factor of four when the distance is doubled (Lakhwani,

Dalal, Jindal, & Nagala, 2019).

Shielding materials can be defined as protective materials to reduce exposure to radiation by the attenuation principle, which is the ability to absorb or attenuate radiation by placing material such as Pb, concrete, or water between the source of radiation and a person. There are several factors that affect the efficiency of radiation shielding, including radiation type and its energy, shielding material effective atomic number, and other parameters. Fig. 2.1 illustrates the types of ionizing radiation and their ability to penetrate. It can be noted that uncharged radiation possesses high penetration power and can travel in the air. On the other hand, they interact with high-density materials such as lead, iron, concrete, and other materials, and they are easy to stop inside them. (Gökçe, Öztürk, Çam, & Andiç-Çakır, 2018).

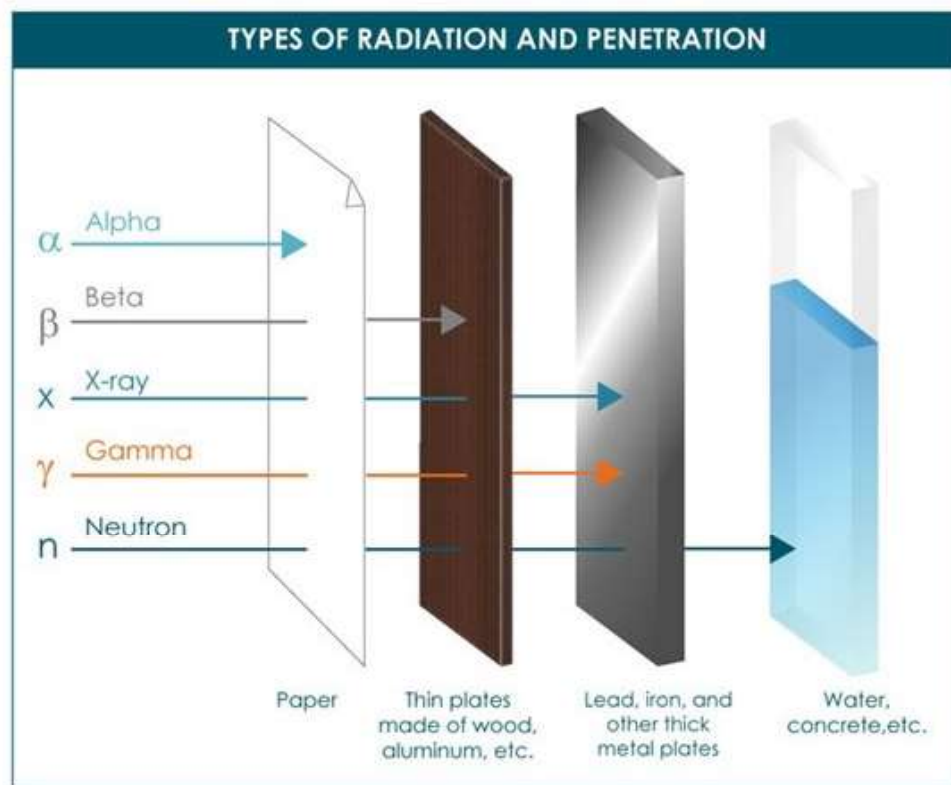


Figure 2.1: Types of radiation and their ability to penetrate (Knoll, 2010).

## 2.1.2 Photons interaction with matter

When photons enter through a medium, part of the photons will be transmitted without interaction with the medium, while other photons will interact with the atoms or molecules of the material, causing their energy to be absorbed or scattered (Knoll, 2010). The main processes that may occur when the photons interact with the medium are the photoelectric effect ( $\sigma_f$ ), Compton effect ( $\sigma_C$ ), and pair production ( $\sigma_p$ ). Fig. 2.2 illustrates the energy range and atomic number where the photoelectric effect, the Compton effect, and pair production are dominant.

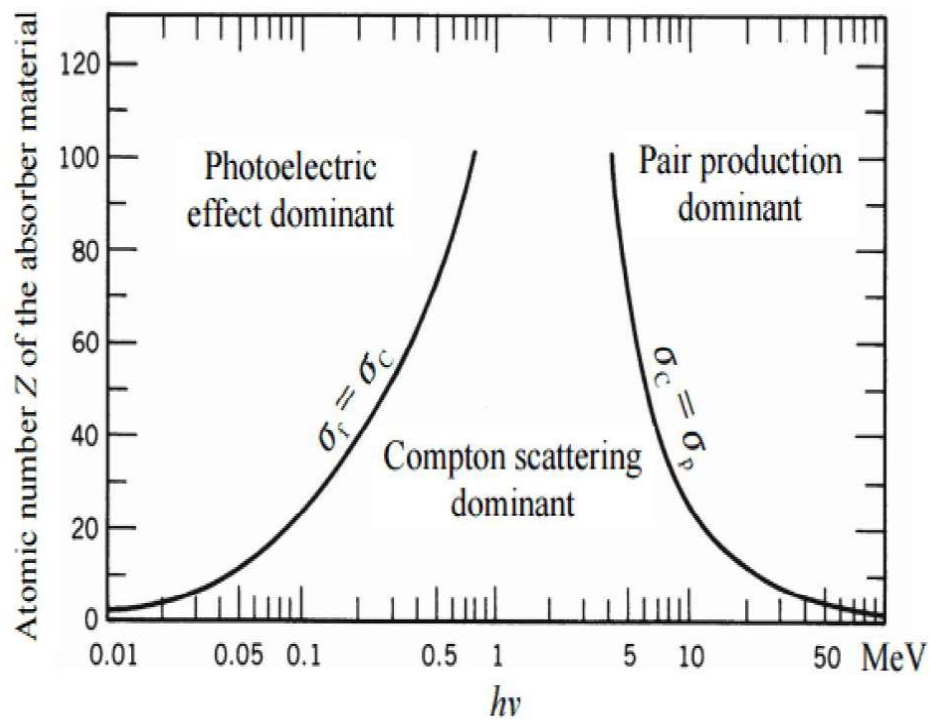


Figure 2.2: The three major types of radiation interactions with matter (Knoll, 2010).

### **2.1.2(a) The photoelectric effect**

The photoelectric effect occurs at a low energy region between the incident photons and the electrons of the absorbing atom where the interaction causes the complete disappearance of the photon, and the electron is ejected into the medium from the inner electron shell like a K-shell. The interaction also produces a vacancy in the orbit of absorbed atoms. By capturing the free electron from the medium or rearrangement of the electrons from the outer shell, the atom fills the vacancy. When the vacancy is filled, X-ray is emitted, or in some cases, the Auger electron is emitted instead of the X-ray. The photoelectric effect is proportional to the atomic number of absorbing materials and inversely proportional to photon energy. At lighter elements, the photoelectric effect energy range of around 10 keV dominates, while the energy range for heavy elements is around 1 MeV as shown in Fig 2.2.

### **2.1.2(b) Compton scattering**

Compton scattering is the interaction between photons and outer shell electrons of absorbing materials where the photon strikes the outer shell electron, causing the photon to transfer part of its energy to the electron and change direction to move in the new direction while the electron is ejected from its orbit. The Compton scatter decreases gradually with increasing photon energy and increases linearly with atomic number. Figure 2.2 shows that the Compton scattering energy range (10 keV to 10 MeV) dominates in lighter elements. While the energy range for heavy metals (1-4 MeV).

### **2.1.2(c) Pair production**

Pair production is one of the mechanisms that can convert radiation to matter in high energy regions. If the photon energy exceeds twice the rest mass of a single electron (1.02 MeV), the photons interact with the electric field of the target nuclei of absorbing materials, causing the photon to disappear and producing a positron-electron pair. Pair production is predominantly confined to high-energy gamma rays. The probability of this interaction remains very low until the gamma-ray energy approaches several MeV. This happens when the energy of the gamma rays is above 10 MeV for lighter elements and above 4 MeV for heavier elements, as shown in Fig 2.2.

## **2.2 The glass as radiation shielding material**

One of the conventional methods utilized for nuclear radiation shielding is concrete which is cheap and easy to shape for any design. However, it has disadvantages, such as considerable opaque to visible light, thus, restricting worker or onlookers to see through it, water permeability, and its mechanical strength is reduced when the concrete is exposed to radiation for a long period. The glass materials are considered alternative to concrete as radiation shielding since they can be visible light transparent and their properties and structure can be changed by adding some materials and heat treatment to be able to absorb gamma rays (Sayyed, Kaky, Gaikwad, et al., 2019).

Glass structures contain three important compounds: formers, modifiers, and intermediates. The glass former is the glass backbone, and it is used to create glass

networks such as borate, silicate, borosilicate, etc . Borosilicate glass formers possess enticing characteristics such as low coefficient of thermal expansion which make them more resistant to thermal shock than other commercial glasses. Also, they have excellent transmission of visible light (Bootjomchai, Laopaiboon, Yenchai, & Laopaiboon, 2012; Chanthima & Kaewkhao, 2013). Heavy metal oxides such as PbO, BaO, Bi<sub>2</sub>O<sub>3</sub>, MoO<sub>3</sub>, WO<sub>3</sub>, and others in glass networks for use as glass shielding can be used because they possess desirable features such as high density, strong nonlinear optical susceptibility, and excellent  $\gamma$ -ray shielding. Bismuth(III) oxide (Bi<sub>2</sub>O<sub>3</sub>) and barium oxide (BaO) are used in shielding materials for protection against radiation and to develop radiation shielding glass. There are a substitute for PbO which is toxic. Bi<sub>2</sub>O<sub>3</sub> has desirable features, such as high values of optical susceptibility, optical basicity, polarizability, refractive index, density, and effective atomic number, which provide Bi<sub>2</sub>O<sub>3</sub> with a high attenuation capability (Elsafi, El-Nahal, Sayyed, Saleh, & Abbas, 2021; Kaewkhao, Pokaipisit, & Limsuwan, 2010; Yasaka, Pattanaboonmee, Kim, Limkitjaroenporn, & Kaewkhao, 2014). Tungsten trioxide (WO<sub>3</sub>) has attracted great attention in many fields due to its properties, such as being non-toxic and its ability to absorb gamma rays because of its high density and higher atomic number. Furthermore, it has six different states: 0, +2, +3, +4, +5, and +6, but in glass, WO<sub>3</sub> can be found at W<sup>+3</sup>, W<sup>+4</sup>, W<sup>+5</sup>, and W<sup>+6</sup> (Issa, Rashad, Hanafy, & Saddeek, 2020; Mostafa, Issa, & Sayyed, 2017). Zinc oxide (ZnO) has a significant impact on glass formation capability and reduces crystallization rates in the glass network (Alazoumi et al., 2017).

Researchers have focused on the preparation of heavy metal oxide glasses. Stalin et al. (2021) fabricated lithium bismuth boro-tungsten glasses to investigate gamma

ray shielding features. Aboalatta et al. (2021) investigated the gamma-ray shielding features of sodium zinc borate glasses doped with different concentrations of barium oxide. Sallam, Madbouly, Elalaily, and Ezz-Eldin (2020) prepared bismuth borate glasses doped 0.7% of one of the following transition metals (Cu,Co, and Ni) to enhance these glasses as gamma ray shielding material. P. Kaur, Singh, Thakur, Singh, and Bajwa (2019) fabricated bismuth borate glass system modified with barium to explore the possibility of replacing lead for application as gamma-ray shielding materials. Sayyed, Kaky, Gaikwad, et al. (2019) doped heavy metals such as  $\text{Bi}_2\text{O}_3$  and  $\text{MoO}_3$  into borate glasses to develop new glass shielding against radiation.

### 2.3 Radiation shielding parameters

The attenuation principle is the reduction of a photon's intensity through the medium via scattering or absorption. When the photon moves through the medium, three major processes may occur: photoelectric effects ( $\tau$ ), Compton scattering ( $\sigma$ ), and pair production ( $\kappa$ ). The sum of the probabilities of these processes is called the linear attenuation coefficient( $\mu$ ) (Knoll, 2010).

$$\mu = \tau(\text{photoelectric}) + \sigma(\text{Compton}) + \kappa(\text{pair}) \quad (2.1)$$

#### 2.3.1 Linear Attenuation coefficient(LAC).

Attenuation of gamma-rays is an important factor in determining the shielding properties of the glasses. It is described as the fraction of photons that are absorbed or scattered per unit thickness of the material. It is dependent on the density and

composition sample materials and can be expressed using Lambert-Beer law (M. Ç. Ersundu, Ersundu, Sayyed, Lakshminarayana, & Aydin, 2017).

$$I = I_0 e^{-\mu x} \quad (2.2)$$

Where  $I$  is the intensity of gamma-ray photons transmitted through some distance  $x$ ,  $I_0$  is the initial intensity of gamma-ray photons,  $\mu$  is the linear attenuation coefficient, and  $x$  is the thickness of the glass samples.

Many researchers studied the LAC to estimate other attenuation parameters and determine glass shielding properties. Sadeq et al. (2022) compared the measured linear attenuation coefficients with those simulated via Geant4 code and computed by XCOM software for borosilicate glassy systems doped with mixed heavy metals. They found that the values of both linear coefficients increased as the  $\text{Bi}_2\text{O}_3$  concentration increased. Also, Aladailah et al. (2022) measured the linear attenuation coefficient of glass systems with the system of  $45 \text{ SiO}_2-15 \text{ CaO}-(40-x) \text{ BaO} - (x) \text{ ZnO}$  (where  $x = 0, 10, 20, 30,$  and  $40 \text{ wt}\%$ ) using XCOM software and Geant4 simulation in the energy range of  $0.0595 \text{ MeV}-1.410 \text{ MeV}$  and using a narrow beam using the NaI(Tl) scintillation detector at different energies. They confirmed that there have been good agreements.

### **2.3.2 Mass attenuation coefficient(MAC).**

One of the simplest parameters that can be used to understand the absorption ability of the glass samples for incident photons is the mass attenuation coefficient

( $\mu_m$ ). It is the probability of the interaction that occurs between gamma-ray photon and glass samples of the unit mass per unit area, and it has quantities  $\text{cm}^2\text{g}^{-1}$  (Sayyed, Issa, Tekin, & Saddeek, 2018). According to Lambert-Beer law, the mass attenuation coefficient of investigated materials is calculated experimentally.

$$\mu_m = \frac{\ln(\frac{I_0}{I})}{\rho x} \quad (2.3)$$

On the other hand, the theoretical value of mass attenuation coefficient of mixture or compound has been calculated using simulation programmes such as XCOM, Monte Carlo, PhysX/PDS online software, and other programmes.

$$\mu_m = \sum_i w_i (\mu_m)_i \quad (2.4)$$

Where  $(\mu_m)_i$  is the mass attenuation coefficient for individual components and,  $w_i$  is the weight fraction of the component in the compound.

El-Denglawey et al. (2021) measured the linear and mass attenuation coefficients and other shielding parameters of glass containing bismuth using Monte Carlo simulation and the XCOM program. The glass composition was  $x\text{Bi}_2\text{O}_3-(75-x)\text{B}_2\text{O}_3-25\text{Li}_2\text{O}$  ( $x = 0, 10, 20, 30, 40, 50, 60$  the  $70$  mol%). They found that the LAC and MAC values decreased as photon energy was increased, as seen in Figures 2.3 and 2.4, respectively. Furthermore, N. S. Ahmad et al. (2018) investigated the radiation shielding properties of bismuth and lead doped into SLS glasses experimentally at energies of 0.059, 0.122, and 0.662 MeV. They discovered that the

linear and mass attenuation coefficients decreased as gamma energy increased. The results are consistent with a number of studies which are (Sayyed, Ersundu, Ersundu, Lakshminarayana, & Kostka, 2018), (M. Ç. Ersundu et al., 2017), (Kaundal, 2016), and (N. Singh, Singh, Singh, & Singh, 2004).

Almuqrin and Sayyed (2021) examined the attenuation properties of the  $\text{Bi}_2\text{O}_3\text{-WO}_3\text{-TeO}_2$  glass and  $\text{PbO-WO}_3\text{-TeO}_2$  glass. Their results showed that the glass samples that contained high levels of  $\text{WO}_3$  and  $\text{Bi}_2\text{O}_3$  possessed the best attenuation, and they also suggested the possibility of using  $\text{Bi}_2\text{O}_3$  and  $\text{WO}_3$  instead of  $\text{PbO}$ . Al-Hadeethi and Sayyed (2019a) compared the effects of  $\text{Bi}_2\text{O}_3$ ,  $\text{BaO}$ , and  $\text{TiO}_2$  on the shielding properties of borosilicate glass. They referred that the glass

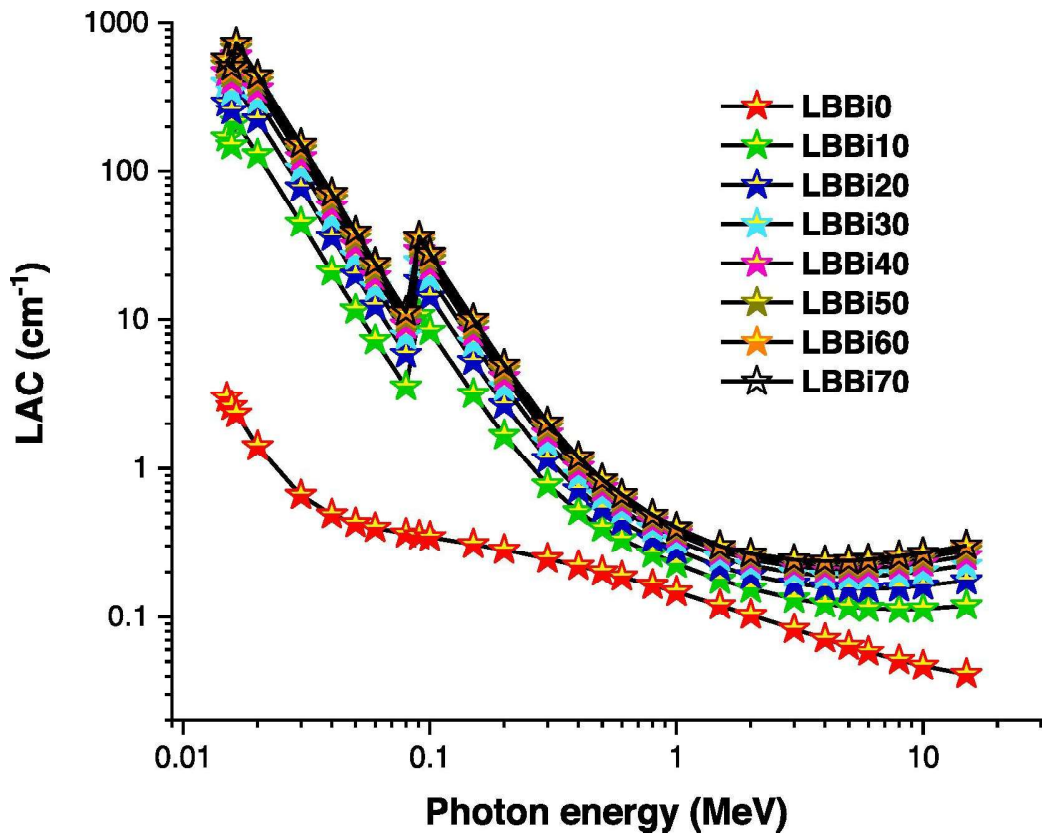


Figure 2.3: Variation of linear attenuation coefficient (LAC) with photon energy (El-Denglawey et al., 2021)

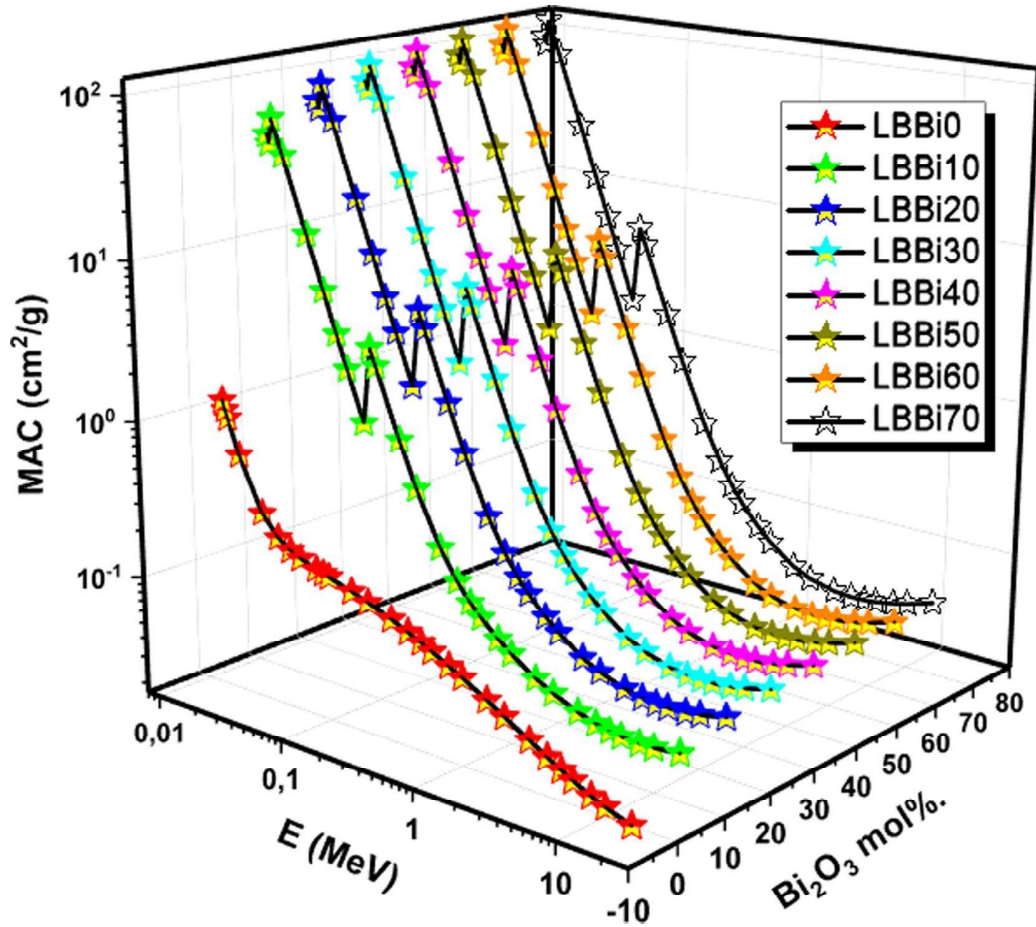


Figure 2.4: Variation of mass attenuation coefficient (MAC) values for the glass samples with photon energy (El-Denglawey et al., 2021).

containing  $\text{Bi}_2\text{O}_3$  had higher values of attenuation compared to  $\text{BaO}$  and  $\text{TiO}_2$  glasses.

Sayyed et al. (2022) studied the shielding parameters of ( $\text{BaO-MoO}_3\text{-B}_2\text{O}_3$ ) glass experimentally using the sources ( $^{137}\text{Cs}$  and  $^{166}\text{Ho}$ ) and theoretically utilizing the XCOM program. They confirmed that all of their results, both theoretical and experimental, were compatible. Moreover, A. Ersundu, Büyükyıldız, Ersundu, Şakar, and Kurudirek (2018) compared the attenuation parameter values of heavy metal oxide glasses experimentally and theoretically using the WinXCom programme. They found that the theoretical results are in good agreement with empirical results.

Sayyed, Mahmoud, et al. (2021) compared the radiation shielding parameters of borate glass containing MoO<sub>3</sub> theoretically between Monte Carlo and XCOM. They referred that the results from both Monte Carlo and XCOM were convergent. While. Khattari and Al-Buriahi (2022) used Monte Carlo simulations and Phy-X/PSD software to examine the attenuation parameters. They discovered that the findings were in remarkable agreement.

### **2.3.3 Half-Value layer (HVL) and mean free path (MFP)**

The idea of Half-Value layer(HVL) is used to measure a photon's ability to penetrate the glass sample . It is defined the thickness of a sample required to diminish the intensity of photon into half of its initial intensity. The HVL is determined as following Eq (Sayyed, Issa, et al., 2018) .

$$HVL = \frac{0.693}{\mu} \quad (2.5)$$

The mean free path is the average distance which a photon travels in the medium before an interaction occurs and can be described depending on the formula (Sayyed, 2017).

$$MFP = \frac{1}{\mu} \quad (2.6)$$

Many researchers calculate the HVL and MFP depending on linear attenuation

values of glass samples. One of these researchers is Abouhaswa, Sayyed, et al. (2020). They observed the HVL and MFP values increased as the photon energy increased, as depicted in Fig. 2.5. Numerous other research have shown similar outcomes, such as (Kumar et al., 2020), (Cheewasukhanont et al., 2021), and (A. Ersundu et al., 2018).

According to D’Souza et al. (2021), who found that the HVL and MFP values were reduced as  $\text{Bi}_2\text{O}_3$  content was raised in the glass network. As well, El-Sharkawy et al. (2020) observed that the HVL and MFP decreased when the NiO content increased. Kirdsiri, Kaewkhao, Chanthima, and Limsuwan (2011) derived HVL of silicate glass systems containing ( $\text{Bi}_2\text{O}_3$ , PbO, and BaO). They found  $\text{Bi}_2\text{O}_3$  and BaO can be used

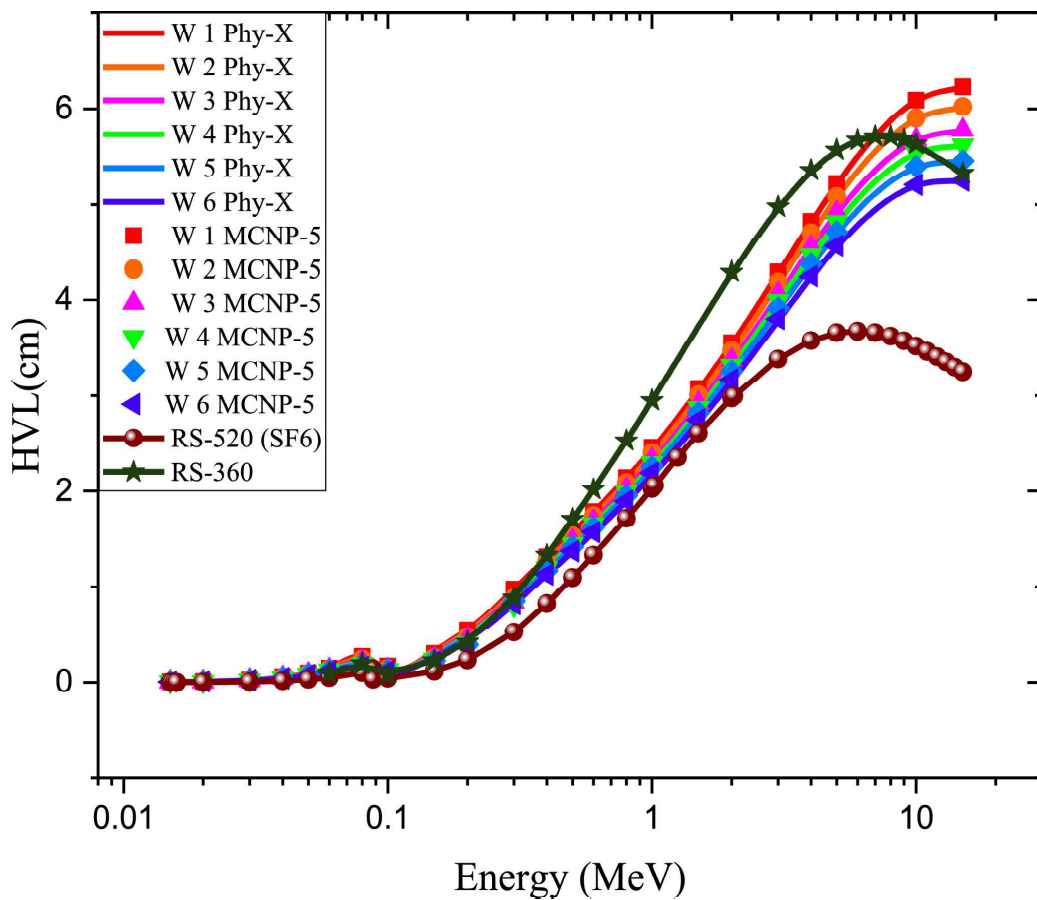


Figure 2.5: The HVL of the fabricated glasses with photon energy (Abouhaswa, Sayyed, et al., 2020)

as lead-free radiation shielding without toxicity to our environmental.

#### 2.3.4 The effective atomic number( $Z_{eff}$ ) and electron density ( $N_{el}$ )

The effective atomic number( $Z_{eff}$ ) are considered a very useful parameter for mixture materials such as glass due to  $\mu_m$  depended on  $Z_{eff}$  and is computed using formulas (Kavaz, Tekin, Yorgun, Özdemir, & Sayyed, 2019).

$$Z_{eff} = \frac{\sigma_{t,a}}{\sigma_{t,el}} \quad (2.7)$$

Where  $\sigma_{t,a}$  and  $\sigma_{t,el}$  are atomic cross-section and electronic cross-section respectively. Atomic-cross section is computed using the following formula.

$$\sigma_{t,a} = \frac{\mu_m}{N_A \sum_i \frac{w_i}{A_i}} \quad (2.8)$$

Where  $A_i$  and  $N_A$  are the atomic weight of the  $i^{th}$  element in the composition materials and Avogadro's number respectively. Where as, electronic cross-section is calculated depending on the next formula:

$$\sigma_{t,el} = \frac{1}{N_A} \sum_i \frac{f_i A_i}{Z_i} (\mu_i) \quad (2.9)$$

Where ( $f_i$ ) is number of the atoms of element  $i$  relative the total number of atoms of all elements in the alloy, and ( $Z_i$ ) is the atomic number of the  $i^{th}$  element in the alloy.

The electron density ( $N_{el}$ ) is the number of electrons per unit mass and is written as follows: (Chanthima et al., 2017).

$$N_{el} = \frac{\mu_m}{\sigma_{t,el}} \quad (2.10)$$

Teresa et al. (2021) doped heavy metal ions into calcium borotellurite glass and measured the effective atomic number values using phys-X software at an energy range of 0.2 to 1.4 MeV. They detected that the  $Z_{eff}$  decreased as photon energy increased as shown in Fig. 2.6. A. Ersundu et al. (2018) mentioned that the ability of a glass shield to attenuate radiation goes up when its effective atomic number increases. This is because the atomic number is proportional to the number of electrons in the atoms. Also, Issa (2016) mentioned that the  $Z_{eff}$  and  $N_{el}$  were increased as the heavy metal oxide content in the glass structure was increased. The results are consistent with studies which are (A. Ali, El-Khayatt, & Akkurt, 2016) and (V. P. Singh, Badiger, & Kaewkhao, 2014).

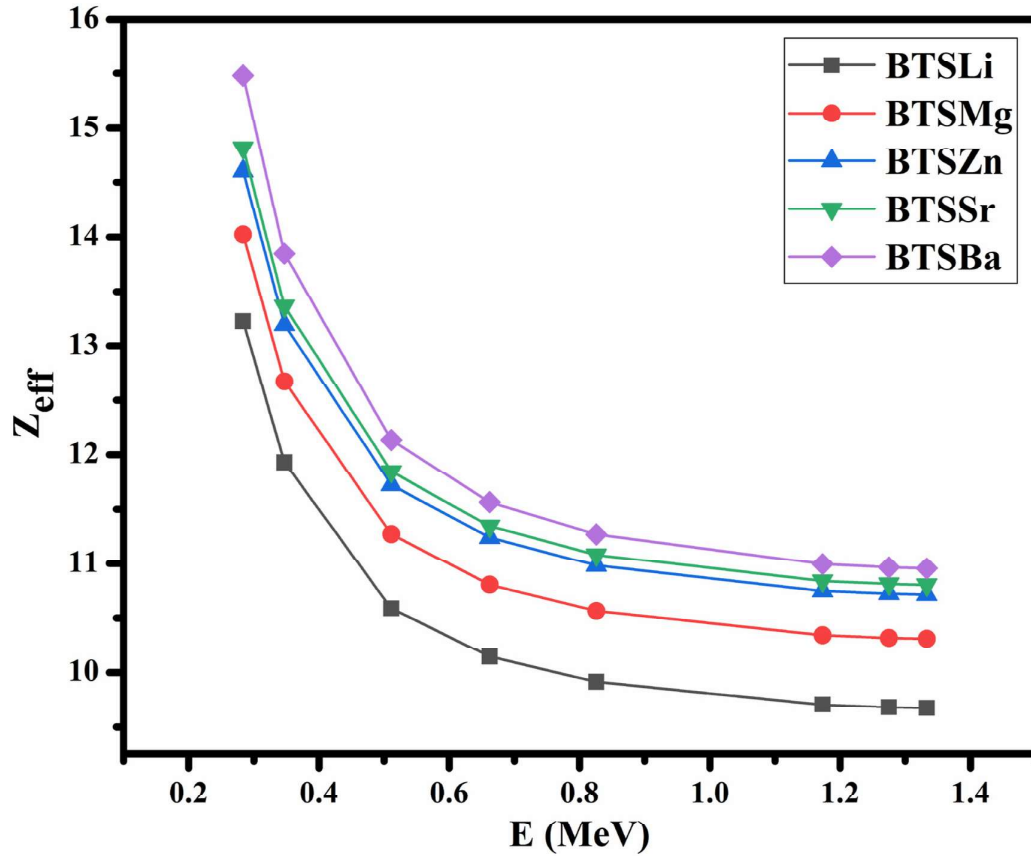


Figure 2.6: The effective atomic number of the glass samples against incoming photon energy. (Teresa et al., 2021)

### 2.3.5 Radiation protection efficiency (RPE)

One of the main attenuation parameters that the researchers are interested in studying when designing the radiation shielding materials is radiation protection efficiency (RPE), which is written as (Kumar, 2017).

$$RPE(\%) = \left(1 - \frac{I}{I_0}\right) \times 100 \quad (2.11)$$

Where  $I$  is the intensity of gamma-ray photons transmitted through glass,  $I_0$  is the

initial intensity of gamma-ray photons transmitted without glass.

Al-Hadeethi, Sayyed, and Nune (2021) prepared a glass shield of  $\text{WO}_3$  doped in borate glass in order to study the attenuation properties of glass using Genta 4 code and Phys-X software. They noted that the radiation protection efficiency (RPE) values of glass samples were increased with glass thickness being increased and  $\text{WO}_3$  content being increased. Also, Almuqrin, Sayyed, Prabhu, and Kamath (2022) computed the RPE values of lithium zinc bismuth silicate glass using Phys-X software. They found RPE values improved from 23–73% when the glass thickness was increased from 0.2 to 1 cm.

#### **2.4 Attenuation study in theoretically approach**

Simulation technology is used to study the radiation attenuation and parameters related to the attenuation of shielding materials. This method aims to save time and reduce costs in applying experiments. In addition, it aims to improve the accuracy of the results. In the theoretical approach, XCOM, WinXCOM, XMuDat, Geant4 Monte Carlo simulations, Phys-X/SPD software, and other programmes are used to figure out the attenuation parameters.

One of the oldest software packages which is used to calculate the radiation mass attenuation coefficients of defined samples is the XCOM software. It is an easy-to-use programme that is easily accessible via the internet. However, it does not compute other shielding parameters, such as linear attenuation coefficient. Another example of simulation software is the Phys-X/SPD software. This software has many benefits, such as being easy to use and free to find online. It can also calculate all shielding

parameters with high accuracy and quickly (Şakar, Özpolat, Alım, Sayyed, & Kurudirek, 2020).

Khattari and Al-Buriahi (2022) evaluated the attenuation parameters of BaO–ZnO–La<sub>2</sub>O<sub>3</sub>–Al<sub>2</sub>O<sub>3</sub>–B<sub>2</sub>O<sub>3</sub>–SiO<sub>2</sub> glasses using XCOM, Geant4 software, and the Phy-X/PDS programs. They confirmed that the attenuation results in the software used were in excellent agreement. Sayyed, Almuqrin, et al. (2021) used EPICS2017 and PhyX/PSD software to evaluate the shielding characteristics of P<sub>2</sub>O<sub>5</sub>-Nb<sub>2</sub>O<sub>5</sub>-Bi<sub>2</sub>O<sub>3</sub> glass. The authors concluded that the comparison results between EPICS2017 and PhyX/PSD results were close. Also, Alalawi (2020) compared the radiation shielding capabilities of Bi<sub>2</sub>O<sub>3</sub>-Na<sub>2</sub>O-B<sub>2</sub>O<sub>3</sub>-Cu<sub>2</sub>O glasses using the FLUKA code and the Phy-X software. The mass attenuation coefficient results in the two software were close in the low energy region, while in the other energy regions there were acceptable differences between the two approaches.

## **2.5 Study of Soda Lime Silica (SLS) Glass**

SLS glass is one of the most common varieties of conventional glass and is used in many applications with a production rate of above 80%, such as windows, containers, tableware, and insulating materials. It can be used in many industries because of its low melting point, chemical and electrical and mechanical resistance, transmission of visible light, and inexpensive manufacturing costs (Kurtulus & Kavas, 2020; Kurtulus et al., 2021). SLS glass is composed of SiO<sub>2</sub>, Na<sub>2</sub>O, CaO, Al<sub>2</sub>O<sub>3</sub>, MgO, and other elements. Shelby (2020) referred to the components of commercial SLS glass models; the windows are composed of 73% SiO<sub>2</sub>, 14% Na<sub>2</sub>O, 9% CaO, 4% MgO,